

Atomic-Scale Structural Evolution and Stability of Supercooled Liquid of a Zr-Based Bulk Metallic Glass

Q. Wang,^{1,2} C. T. Liu,^{2,3} Y. Yang,^{2,*} Y. D. Dong,¹ and J. Lu^{3,†}

¹*Institute of Materials Science, Shanghai University, Shanghai 200072, China*

²*Department of Mechanical Engineering, The Hong Kong Polytechnic University, Hong Kong, China*

³*Department of Manufacturing Engineering and Engineering Management, City University of Hong Kong, Hong Kong, China*

(Received 19 January 2011; revised manuscript received 23 March 2011; published 25 May 2011)

In this Letter, direct experimental evidence is provided for understanding the thermal stability with respect to crystallization in the $\text{Zr}_{41.2}\text{Ti}_{13.8}\text{Cu}_{12.5}\text{Ni}_{10}\text{Be}_{22.5}$ glass-forming liquid. Through high-resolution transmission electron microscopy, the atomic-structure evolution in the glass-forming liquid during the isothermal annealing process is clearly revealed. In contrast with the existing theoretical models, our results reveal that, prior to nanocrystallization, there exists a metastable state prone to forming icosahedra-like atomic clusters, which impede the subsequent crystallization and hence stabilize the supercooled liquid. The outcome of the current research underpins the topological origin for the excellent thermal stability displayed by the Zr-based bulk metallic glass.

DOI: 10.1103/PhysRevLett.106.215505

PACS numbers: 81.05.Kf, 81.40.Ef

Since the advent of multicomponent bulk metallic glasses (BMGs) in the early 1990s, the stability of their glass-forming liquids with respect to crystallization have been extensively investigated owing to its scientific and technological importance [1–14]. Despite substantial dedicated effort, one question yet to be resolved is why some BMGs exhibit a high crystallization resistance while others do not [12,15]. Furthermore, it was observed that, in those BMGs with a superior thermal stability, such as $\text{Zr}_{41.2}\text{Ti}_{13.8}\text{Cu}_{12.5}\text{Ni}_{10}\text{Be}_{22.5}$ (Vit1) [1], high-density nano-sized crystals would be precipitated and well dispersed in the amorphous matrix after annealing. Such a phenomenon is difficult to explain within the classic nucleation theory framework [16,17]; consequently, several theoretical models, which were based on different crystallization scenarios, such as heterogeneous nucleation on impurities or clusters [18,19], a coupled-flux nucleation model [20], and phase separation prior to crystallization [1,2], have been proposed to rationalize the unique features of nanocrystallization in the BMGs. Nevertheless, recent experimental results indicated that the above-mentioned theories cannot fully explain the thermal stability intrinsic to the glass-forming liquids [10,21]. In particular, it has already been found out that phase separation is an unlikely mechanism for the superior stable supercooled liquid as witnessed in the Zr-based BMGs [8]. In such a sense, there appears to be a lack of a unified description which is able to correlate the thermal stability displayed in the glass-forming liquid with the nanocrystallization in BMGs.

In this Letter, we intend to unveil the mechanism for the superior thermal stability against crystallization exhibited by a glass-forming liquid through the investigation of its atomic-structure evolution after annealing. To this end, an amorphous alloy with the chemical composition of $\text{Zr}_{41.2}\text{Ti}_{13.8}\text{Cu}_{12.5}\text{Ni}_{10}\text{Be}_{22.5}$ (in atomic %) was selected

as the model material. According to the differential scanning calorimetry results (see supplemental material [22] for details), the Zr-based alloy was first annealed at 646 K for 1850, 3600, and 7200 s, respectively, and then characterized by x-ray diffraction and high-resolution transmission electron microscopy (HRTEM). The HRTEM observations were performed at 200 kV in a JEOL 2010F microscope. An ion beam milling method was used to prepare the thin foil specimens of the as-prepared and preannealed alloys.

Figures 1(a)–1(d) show the typical HRTEM images and selected area electron diffraction (SAED) patterns taken from an as-prepared sample and samples aged at 646 K for 1850 s, 3600 s, 7200 s, respectively. It is clear that after isothermal annealing up to 3600 s, the Zr-based BMG alloy still remains amorphous, exhibiting a mazelike pattern without any local lattice fringes. This agrees well with the previous x-ray diffraction experimental results (see supplemental material [22]). However, it is likely that atomic-scale ordering may have occurred, which leads to the sharpening of the corresponding SAED patterns with the increasing annealing time (see insets of Fig. 1). For the alloy annealed for 3600 s, even the second ring in the SAED pattern becomes pronounced, indicative of increasing short- (or medium-)range ordering. To reveal such a change in the local atomic structure, Fourier transformation (FT) and inverse Fourier transformation (IFT) were performed on the selected areas of the corresponding HRTEM images, as shown in Fig. 2. In the as-prepared sample, very few icosahedra-like atomic clusters, as marked by the white circle, can be observed [Fig. 2(a)]. In contrast, more and more atomic clusters of a similar type become visible with the increasing annealing time [Figs. 2(b) and 2(c)], which is in line with the change in the SAED patterns in Figs. 2(a)–2(d). With further

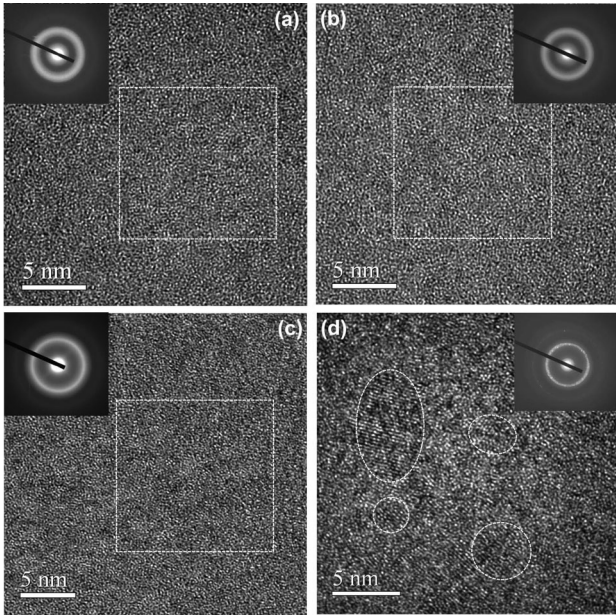


FIG. 1. The HRTEM images with the corresponding selected area diffraction patterns in the insets for the samples (a) in the as-prepared state and isothermally annealed at 646 K for (c) 1850 s, (d) 3600 s, and (e) 7200 s, respectively.

increasing the duration of the isothermal annealing, nanocrystallization in the supercooled liquid of the Zr-based alloy finally occurred. A typical HRTEM image from the sample annealed at 646 K for 7200 s reveals nanocrystallization, as characterized by the lattice fringes dispersed in the remaining amorphous matrix [Fig. 1(d)]. Accordingly, Bragg diffraction dots can be seen superimposed on the amorphous diffuse ring in the corresponding SAED pattern [the inset of Fig. 1(d)].

Based on the above descriptions, it is evident that, to achieve the global structural ordering, the atomic structure of the Zr-based BMG evolves first into a short-ranged icosahedral-like ordered structure at the length scale of 1–2 nm, which resembles spherical symmetry and is well dispersed in the amorphous matrix, and then into the nanocrystalline structure, which is of a long range (> 2 nm) with a translational symmetry. To further reveal such a key stage entailing the transition from the short- to long-range order, Fig. 3 presents a series of FT- and IFT-filtered

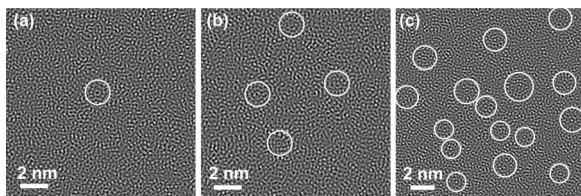


FIG. 2. The typical icosahedral-like atomic ordering in the $Zr_{41.2}Ti_{13.8}Cu_{12.5}Ni_{10}Be_{22.5}$ BMG after isothermally annealing at 646 K. (a–c) are the IFT-filtered images of the selected areas in Fig. 1(a–c), respectively.

images of the atomic structures, which were taken at different areas from the nanocrystallized sample. Owing to the rapid quenching from the annealing temperature, those structural features, as shown in Fig. 3, can be also regarded as the frozen-in “traces” left by the evolving atomic structure at different time steps.

Figure 3(a) presents the atomic structure at the infant stage of nanocrystallization after annealing at 646 K for 7200 s. It can be seen that a number of icosahedral-like atomic clusters aggregate at this stage, exhibiting the characteristics of the so-called imperfect ordering packing as termed in Ref. [23], which was regarded as the embryonic site of crystallization. In Fig. 3(e), two very faint diffraction spots overlapping the diffuse ring can be detected, indicative of the onset of structural transformation, which relates to the atoms as enclosed in the yellow circle being aligned nearly along one dimension. In Fig. 3(b), the feature of the fringe lines characterizing the one-dimensional (1D) translational symmetry becomes more pronounced, which is in line with the two bright spots appearing on the diffraction pattern in Fig. 3(f). Note that some 1D periodic patterns meet the icosahedral-like atomic clusters [marked by the solid circles in Figs. 3(b)–3(d)] at both ends while the others “trap” them inside, which causes lattice distortion as clearly shown in Fig. 3(c). Although short-range ordered atomic clusters have been proposed as the crystallization sites for metallic glasses in the literature [8,11], however, here our experimental results clearly indicate that the atomic clusters act mainly as obstacles to the formation of the global 1D periodicity. The presence of the atomic clusters raises lattice mismatch in the ordered atomic structures, causing delayed crystal nucleation and resulting in a pinning effect,

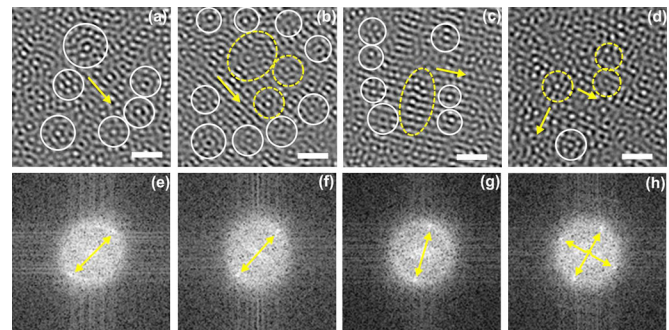


FIG. 3 (color online). The typical localized atomic ordering observed during nanocrystallization of the $Zr_{41.2}Ti_{13.8}Cu_{12.5}Ni_{10}Be_{22.5}$ supercooled liquid at 646 K for 7200 s. (a–d) are the atomic configurations for an amorphous region with ordered clusters. The enclosed areas in (a) show the icosahedral-like clusters, and (b–c) and (d) the ordering clusters in the imperfect 1D and 2D type order packing, respectively. (e–h) are the corresponding FT diffraction patterns (scale bar = 1 nm). Note that the solid (white) and dashed (yellow) circles mark the positions of the atomic clusters close to the boundaries of and within the 1D or 2D type order packing regions, respectively.

which suppresses the growth of crystalline embryos in the amorphous structure.

Indeed, the pinning effect of the atomic clusters has been clearly demonstrated in Figs. 3(a)–3(d). It is noteworthy that the icosahedral-like atomic clusters, which remain nearly unaltered during the early process of crystallization (as enclosed in the solid circles), appear mainly around the boundaries of the long-range ordered structures (1D or 2D). In those places, the translational symmetry terminates and transitions to a disordered structure. On the other hand, the atomic clusters being trapped exhibit a clear morphological transformation from a spherical- to translational-like symmetry, as shown by the dashed ellipse in Fig. 3(c). The curly lattice as compared to the normal 1D periodicity provides the important evidence for the transition from the icosahedral-like atomic clusters to the normal crystalline phase, during which a relatively high energy demand is expected for the breakdown of the atomic clusters. In view of the vivid experimental evidence, the atomic clusters can be pictured as “pinning” the crystals. As a result of the atomic-cluster pinning, crystal growth is hindered and nanocrystallization is therefore promoted in the Zr-based BMG.

The other effect of the atomic clusters on the stability of the Zr-based supercooled liquid is related to the kinetic slowdown of the nucleation process. According to Turnbull [16], the nucleation rate I_s of crystals, which characterizes the stability of a supercooled liquid, can be expressed as $I_s \propto \exp(-\Delta G^*/kT)/\eta$, where η is the viscosity, T is the temperature, k is the Boltzmann constant, and ΔG^* is the effective free-energy barrier for the nucleation of a critical nucleus and can be simply written as $\Delta G^* \propto \sigma^3/(\Delta G + \Delta E)^2$, where σ denotes the interfacial energy between a supercooled liquid and a crystal, ΔG is the free-energy difference between them and the driving force for crystalline nucleation, while ΔE is a positive transformation-induced strain energy opposing crystallization. Obviously, the presence of the icosahedral-like atomic clusters effectively raises the overall viscosity η of the supercooled liquid and σ . Meanwhile, owing to the lattice mismatch, ΔE is elevated, which further reduces the nucleation rate of crystals out of an amorphous structure.

Both effects of the atomic clusters can be illustrated in Fig. 4. While the common notion from the classic theory adopts a “two-well” concept [11,24], in which a disordered structure can be envisaged as jumping across an energy barrier directly into the corresponding crystalline phase, however, our results suggest that it is necessary to add a short-range ordered metastable state in between (Fig. 4). On one hand, the inclusion of such a metastable state leads to the kinetic slowdown of crystal nucleation; on the other hand, the formation of stable atomic clusters greatly reduces the system’s potential and, thus, elevates the energy barrier against crystallization. As those stable atomic clusters with spherical symmetry cannot readily

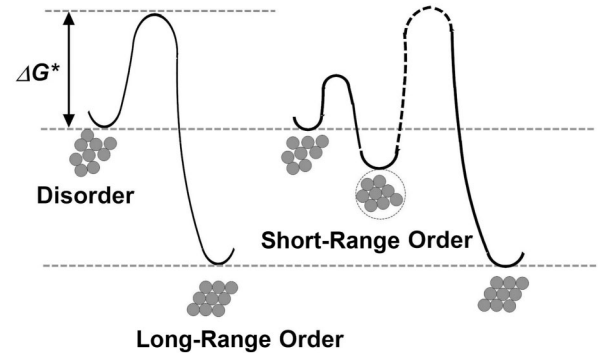


FIG. 4. The schematics of the potential energy profiles for the $\text{Zr}_{41.2}\text{Ti}_{13.8}\text{Cu}_{12.5}\text{Ni}_{10}\text{Be}_{22.5}$ supercooled liquid showing the effect of short-range ordering on subsequent crystallization.

grow in size, they subsequently pin the crystals nucleating nearby and hence promote nanocrystallization in an amorphous structure. Here, it should be stressed that, for effective atomic-cluster pinning, it is critical to have a significant elevation of the energy barrier between the atomic-cluster and crystal states (Fig. 4). In the case that atomic clusters form without significantly lowering the system’s potential, the pinning effect would be impaired. In the BMG literature, there is a long-standing notion that icosahedra-type atomic clusters should play a role of structural “stabilizer” for Zr-based BMGs [25–28]. While this notion was gained previously from atomic simulations, it is consistent with the current experimental findings. Finally, one may ask why the Zr-based BMG prefers to first form the icosahedral-like atomic clusters before directly transforming into crystalline structures. From the topological point of view, this may be related to the packing efficiency in a multicomponent system. With the constituent atoms of distinctly different sizes, it has been shown that the most efficient packing occurs locally in icosahedra-type clusters in the Zr-based BMGs [29]; however, this type of packing cannot be extended readily to form long-range ordering. As a result, the optimization of packing efficiency instead of phase separation leads to the superior crystallization resistance in the Zr-based BMG, as supported by our current experimental findings.

In summary, we have identified the key mechanism in this Letter that leads to the superior thermal stability of the $\text{Zr}_{41.2}\text{Ti}_{13.8}\text{Cu}_{12.5}\text{Ni}_{10}\text{Be}_{22.5}$ BMG which precipitates nanocrystals under annealing. The experimental evidence unambiguously points out that the formation of icosahedral-like atomic clusters with a stable topological packing is vital to achieve the superior thermal stability in the Zr-based BMG. Similar mechanisms may also exist in other types of amorphous alloys which possess superior thermal stability. Furthermore, our study provides a physical mechanism for the formation of nanocrystals in an amorphous structure which remains a single phase in its supercooled liquid region.

Q. W. would like to thank Dr. X. J. Liu at Hong Kong Polytechnic University (HKPU) for critical discussions and acknowledges the financial support provided by the Natural Science Foundation of China (Grants No. 50871063, No. 50731008) and from the Shanghai Leading Academic Discipline Project (Project No. S30107). Y. Y. and J. L. are thankful to the Hong Kong Research Grant Council (RGC) for the financial support of this research (Grant No. PolyU 5359/09E and CityU8/CRF/08); C. T. L. is grateful for the internal support from HKPU and CityU.

*Corresponding author.

mmyyang@polyu.edu.hk

†Corresponding author.

jianlu@cityu.edu.hk

- [1] S. Schneider, P. Thiyagarajan, and W. L. Johnson, *Appl. Phys. Lett.* **68**, 493 (1996).
- [2] J. F. Loffler and W. L. Johnson, *Appl. Phys. Lett.* **76**, 3394 (2000).
- [3] W. H. Wang, Q. Wei, and S. Friedrich, *Phys. Rev. B* **57**, 8211 (1998).
- [4] Y. X. Zhuang, W. H. Wang, Y. Zhang, M. X. Pan, and D. Q. Zhao, *Appl. Phys. Lett.* **75**, 2392 (1999).
- [5] L. Q. Xing, T. C. Hufnagel, J. Eckert, W. Loser, and L. Schultz, *Appl. Phys. Lett.* **77**, 1970 (2000).
- [6] E. Pekarskaya, J. F. Loffler, and W. L. Johnson, *Acta Mater.* **51**, 4045 (2003).
- [7] X. P. Tang, J. F. Loffler, W. L. Johnson, and Y. Wu, *J. Non-Cryst. Solids* **317**, 118 (2003).
- [8] I. Martin, T. Ohkubo, M. Ohnuma, B. Deconihout, and K. Hono, *Acta Mater.* **52**, 4427 (2004).
- [9] A. A. Kündig, M. Ohnuma, T. Ohkubo, and K. Hono, *Acta Mater.* **53**, 2091 (2005).
- [10] H. Tanaka, *J. Non-Cryst. Solids* **351**, 678 (2005).
- [11] X. J. Liu, G. L. Chen, H. Y. Hou, X. Hui, K. F. Yao, Z. P. Lu, and C. T. Liu, *Acta Mater.* **56**, 2760 (2008).
- [12] A. Inoue, *Acta Mater.* **48**, 279 (2000).
- [13] A. Hirata, Y. Hirotsu, K. Amiya, and A. Inoue, *Phys. Rev. B* **78**, 144205 (2008).
- [14] S. Venkataraman, H. Hermann, C. Mickel, L. Schultz, D. J. Sordelet, and J. Eckert, *Phys. Rev. B* **75**, 104206 (2007).
- [15] Z. P. Lu, C. T. Liu, and Y. D. Dong, *J. Non-Cryst. Solids* **341**, 93 (2004).
- [16] D. Turnbull, *Contemp. Phys.* **10**, 473 (1969).
- [17] K. Lu, *Mater. Sci. Eng. R Rep.* **16**, 161 (1996).
- [18] C. Fan, C. F. Li, A. Inoue, and V. Haas, *Appl. Phys. Lett.* **79**, 1024 (2001).
- [19] C. T. Liu, M. F. Chisholm, and M. K. Miller, *Intermetallics* **10**, 1105 (2002).
- [20] K. F. Kelton, *Philos. Mag. Lett.* **77**, 337 (1998).
- [21] H. Assadi and J. Schroers, *Acta Mater.* **50**, 89 (2002).
- [22] A similar mechanism of icosahedral cluster pinning has also been identified in the Cu₄₆Zr₄₅Al₇Y₂ metallic glass. See supplemental material at <http://link.aps.org/supplemental/10.1103/PhysRevLett.106.215505> for details.
- [23] G. L. Chen, X. J. Liu, X. D. Hui, H. Y. Hou, K. F. Yao, C. T. Liu, and J. Wadsworth, *Appl. Phys. Lett.* **88**, 203115 (2006).
- [24] X. J. Liu, G. L. Chen, X. D. Hui, H. Y. Hou, K. F. Yao, and C. T. Liu, *J. Appl. Phys.* **102**, 063515 (2007).
- [25] Y. Q. Cheng, E. Ma, and H. W. Sheng, *Phys. Rev. Lett.* **102**, 245501 (2009).
- [26] H. W. Sheng, Y. Q. Cheng, P. L. Lee, S. D. Shastri, and E. Ma, *Acta Mater.* **56**, 6264 (2008).
- [27] M. W. Chen, I. Dutta, T. Zhang, A. Inoue, and T. Sakurai, *Appl. Phys. Lett.* **79**, 42 (2001).
- [28] W. K. Luo, H. W. Sheng, F. M. Alamgir, J. M. Bai, J. H. He, and E. Ma, *Phys. Rev. Lett.* **92**, 145502 (2004).
- [29] H. W. Sheng, W. K. Luo, F. M. Alamgir, J. M. Bai, and E. Ma, *Nature (London)* **439**, 419 (2006).